

# Structural Analysis of Oriented Poly( $\epsilon$ -Caprolactone) Including $\text{CaCO}_3$ Particles with $^{13}\text{C}$ Solid-State NMR

TAKURO ITO,<sup>1</sup> YUJI YAMAGUCHI,<sup>1</sup> HIROTO WATANABE,<sup>1</sup> TETUSO ASAKURA<sup>2</sup>

<sup>1</sup> Department of Operations engineering Toyo Seikan, Ltd, Yokohama, Kanagawa, 230-0047, Japan

<sup>2</sup> Department of Biotechnology, Tokyo University of Agriculture and Technology, Koganei, Tokyo, 184-8588, Japan

Received 19 June 2000; accepted 17 August 2000

**ABSTRACT:** The results of a study of the relation between the oriented structure and drawn Poly( $\epsilon$ -caprolactone) specimens including  $\text{CaCO}_3$  particles and their dynamic mechanical properties are presented. The loss elasticity,  $E''$ , showed almost the same curve for both undrawn sheets and drawn sheets as a function of  $\text{CaCO}_3$  content. On the other hand, the storage modulus,  $E'$ , of drawn sheets increased nonlinearly with increasing  $\text{CaCO}_3$  content, and their curve showed lower  $E'$  values than those of undrawn sheets. By simulation of  $^{13}\text{C}$  CP NMR spectra of drawn PCL/ $\text{CaCO}_3$  sheets, both oriented and unoriented components were observed. The distribution parameter,  $p$ , of drawn PCL/ $\text{CaCO}_3$  sheets was  $13^\circ$ , which was larger than those ( $8^\circ$ ) of drawn PCL. Further, the fraction of the unoriented component increased with increasing  $\text{CaCO}_3$  content. Thus, adding  $\text{CaCO}_3$  particles into the PCL, the arrangement of the oriented component was disturbed and decreased. In addition, from the line shape analyses of  $^{13}\text{C}$  CP MAS NMR spectra, four peaks were obtained in not only undrawn sheets but also in drawn sheets of both PCL and PCL/ $\text{CaCO}_3$  compounds. Besides, structural change occurred at only drawn PCL/ $\text{CaCO}_3$  sheets. Therefore, the change in dynamic mechanical properties observed only for drawn PCL/ $\text{CaCO}_3$  sheets were strongly dependent on the orientational structure, which was formed under shear stress of the stretching drawn process. © 2001 John Wiley & Sons, Inc. *J Appl Polym Sci* 80: 2376–2382, 2001

**Key words:** poly( $\epsilon$ -caprolactone);  $^{13}\text{C}$  solid-state NMR; orientation; crystalline structure; chemical shift tensor

## INTRODUCTION

Poly( $\epsilon$ -caprolactone) (PCL) is a biodegradable polymer formed by ring-opening polymerization of lactone. This polymer decomposes rapidly and completely in a typical compost environment, which makes it an ideal replacement for nonde-

gradable polymers in numerous applications like yard-waste bags, surgical, and pharmaceutical materials.<sup>1,2</sup>

The crystal structure of PCL has been determined by X-ray diffraction.<sup>3,4</sup> Two types of conformations were reported: one is the planar zigzag conformation, and the other is a slightly distorted nonplanar zigzag conformation. A recent electron diffraction study revealed that the latter conformation is more suitable.<sup>5</sup> Furthermore, the structure of PCL in the solid state has been characterized by  $^{13}\text{C}$  solid state NMR.<sup>6</sup> Kaji and Horii assigned the  $^{13}\text{C}$  CP/MAS NMR spectrum of PCL

---

Correspondence to: T. Asakura.  
Contract grant sponsor: Bio-oriented Technology Advancement Institute.

*Journal of Applied Polymer Science*, Vol. 80, 2376–2382 (2001)  
© 2001 John Wiley & Sons, Inc.

on the base of the assignment of the solution  $^{13}\text{C}$  NMR and relaxation studies. The  $^{13}\text{C}$  spin-lattice relaxation time analyses revealed that the PCL sample contains three components with different  $T_{1C}$  values, which were assigned to the crystalline, mobile crystalline, and noncrystalline components. By analyzing the  $^{13}\text{C}$  spin-spin relaxation times ( $T_{2C}$ ), it was found that the noncrystalline component can be further resolved into the crystalline–amorphous interfacial and amorphous components. The fractions of the crystalline, interfacial, and amorphous components were finally determined to be 0.42, 0.30, and 0.28, respectively. A detailed discussion of the molecular motion of the crystalline region of PCL chains was also given.

However, the glass transition temperature ( $T_g$ ) and melting temperature ( $T_m$ ) of PCL are very low, that is,  $-60^\circ\text{C}$  and  $60^\circ\text{C}$ , respectively. Therefore, to improve the mechanical properties, the addition of environmentally benign materials such as Calcium Carbonate ( $\text{CaCO}_3$ ), silica, and clay to PCL is generally required for industrial applications. The increase in mechanical strength and biodegradability for PCL/clay and PCL/ $\text{CaCO}_3$  mixtures have been reported.<sup>7,8</sup> However, there have been no studies on the structure of PCL in the solid state of these mixture samples.

In this article, we reported the structure of oriented PCL as a function of  $\text{CaCO}_3$  content determined with  $^{13}\text{C}$  CP MAS and  $^{13}\text{C}$  CP solid-state NMR. The solid-state NMR analytical methods applied for Poly(ethylene terephthalate)<sup>9</sup> and Poly(L-lactic acid)<sup>10</sup> were used in this study. Especially, the relationship between the change in dynamic storage modulus,  $E'$ , of the oriented samples with the heterogeneous structure was investigated.

## EXPERIMENTAL

### Materials

A commercial sample of Poly( $\epsilon$ -caprolactone) (PCL H-7) with  $d = 1.16 \text{ g/cm}^3$  was purchased from Dicel Kagaku Kogyo Ltd (Japan).  $\text{CaCO}_3$  particles with an average particle size of  $1.25 \mu\text{m}$ , used for the dispersed particles, were purchased from Shiraishi Calcium Ltd (Japan).

$\text{CaCO}_3$  and PCL were mixed in a two-roll mill (Toyo Seiki Ltd), at  $140^\circ\text{C}$  for 10 min. The samples for elastic modulus observation,  $^{13}\text{C}$  CP NMR observation and  $^{13}\text{C}$  CP MAS observation were

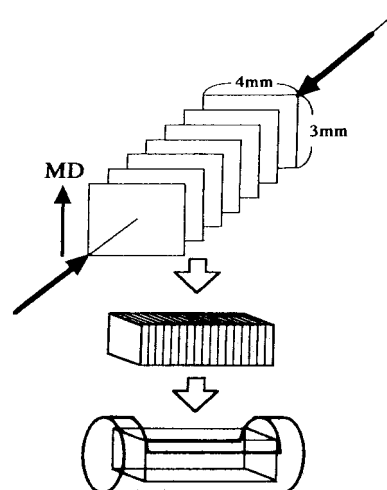


**Figure 1** Preparation of a uniaxially oriented block sample of PCL/ $\text{CaCO}_3$  sheet for  $^{13}\text{C}$  CP NMR observation as a function of  $\beta_L$ , the angle between the machine draw direction (MD) and the magnetic field.

prepared by mold pressing at  $150^\circ\text{C}$  under a pressure of 10 Mpa to form a sheet of 1.0 mm in thickness and then cut into rectangles of dimensions,  $10.0 \times 50.0 \text{ mm}$ . Uniaxially drawn sheets were prepared with a draw rate of 100 mm/min and a draw ratio of 4.5 at  $50^\circ\text{C}$  by a one-way stretch method using an ORIENTEC tensile tester. Especially, the oriented samples for  $^{13}\text{C}$  CP NMR observation used  $3 \times 4 \text{ mm}$  cut sheets, as shown in Figure 1.

### Dynamic Storage Modulus Measurement

Storage modulus,  $E'$ , and loss elasticity,  $E''$ , were obtained from a Dynamic storage modulus instrument, DDV-25FP Visco-elastic Analyzer manufactured by A&D Ltd, at  $25^\circ\text{C}$  and 11 Hz.

### $^{13}\text{C}$ NMR Measurement

$^{13}\text{C}$  CP MAS NMR observations were performed on a CMX 400 NMR spectrometer operating at 100 MHz at  $25^\circ\text{C}$ . The cross polarization (CP) technique (Hartmann-Hahn-matched condition) with contact time = 7 ms was used with a recycle delay of 3 s. Sample spinning rate was set to be 5 kHz. Typically 20,000 FIDs were accumulated for each spectrum. The chemical shift of the methyl peak of hexamethylbenzene was used as chemical shift reference and converted to 17.3 ppm from TMS. Assuming a Gaussian distribution, line shape analyses of the carbonyl peaks were carried out.

$^{13}\text{C}$  CP NMR observations were performed on a JEOL EX270 NMR spectrometer operating at 67.8 MHz at 25°C. The CP technique (Hartmann-Hahn-matched condition) with contact time = 2 ms was used with a recycle delay of 5 s and a spin-locking field strength of 1.2 mT. Typically 15,000 FIDs were accumulated for each spectrum.

## RESULTS

### Dynamic Mechanical Properties of PCL/ $\text{CaCO}_3$ Compounds

The effect of the  $\text{CaCO}_3$  content on the storage modulus,  $E'$ , and the loss elasticity,  $E''$ , of both undrawn and drawn sheets of PCL/ $\text{CaCO}_3$  are shown in Figures 2 and 3, respectively. The loss elasticity,  $E''$ , (Fig. 2) shows almost the same curve for both of undrawn sheets [Fig. 2(b)] and drawn sheets [Fig. 2(a)] as a function of  $\text{CaCO}_3$  content. These results are similar to those of PCL/Clay blend system.<sup>7</sup> In contrast, the curve of the storage modulus,  $E'$ , of drawn sheets [Fig. 1(a)] is different from the undrawn sheets. The curve of  $E'$  slightly increased with increasing  $\text{CaCO}_3$  content, and showed a plateau region having lower  $E'$  values than those of undrawn sheets [Fig. 1(b)]. At a lower filler content, less than 20 wt %, the storage modulus,  $E'$ , of drawn PCL/ $\text{CaCO}_3$  sheets increased with increasing  $\text{CaCO}_3$  content. At above 20 to 45 wt % of  $\text{CaCO}_3$ , the storage modulus,  $E'$ , showed constant values indepen-

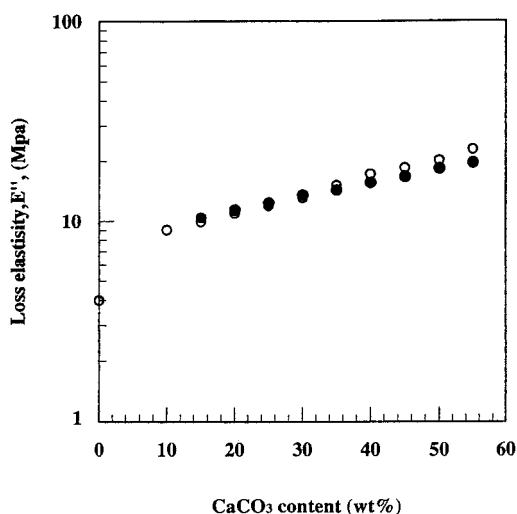


**Figure 2** Storage modulus,  $E'$ , of drawn PCL/ $\text{CaCO}_3$  sheets (●) and undrawn PCL/ $\text{CaCO}_3$  (○) as a function of  $\text{CaCO}_3$  content.

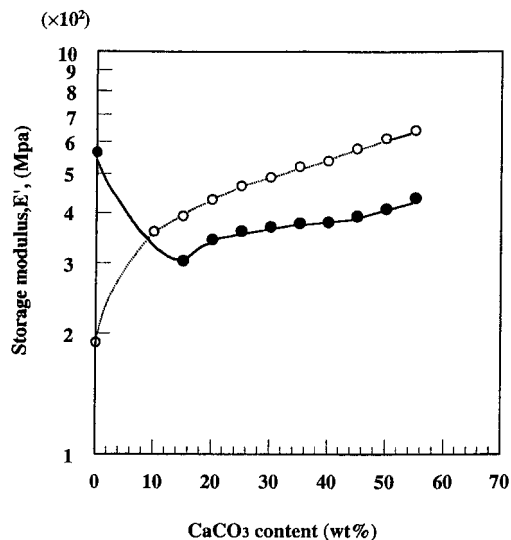


**Figure 3** Loss modulus,  $E''$ , of drawn PCL/ $\text{CaCO}_3$  sheets (●) and undrawn PCL/ $\text{CaCO}_3$  (○) as a function of  $\text{CaCO}_3$  content.

dent of the  $\text{CaCO}_3$  content. At more than 45 wt % of  $\text{CaCO}_3$ , the storage modulus,  $E'$ , slightly increased one more.

Thus, it is clear that some factor that can affect the storage modulus,  $E'$ , occurs under a shear stress during the drawing process of the PCL/ $\text{CaCO}_3$  compounds. There are many factors, such as matrix toughness, interphase adhesion, and particle aggregation, that can affect the storage modulus,  $E'$ , of drawn PCL/ $\text{CaCO}_3$  compounds.

### $^{13}\text{C}$ Solid-State NMR Powder Pattern Spectrum of PCL

In the process of structural analysis of oriented PCL/ $\text{CaCO}_3$  compounds with angle-dependent solid-state NMR, it is necessary to determine the chemical shift tensor values of carbonyl peaks of PCL powder. Figure 4 shows the carbonyl region of the  $^{13}\text{C}$  CP NMR spectrum of the PCL powder sample together with the simulated spectrum. Any carbon peaks due to the calcium carbonate ( $\text{CaCO}_3$ ) could not be observed in the  $^{13}\text{C}$  CP NMR spectrum as is expected from the  $^{13}\text{C}$  CP/MAS NMR spectra, as shown below. After the simulation,<sup>11</sup> the chemical shift tensors were determined to be  $\sigma_{11} = 128$  ppm,  $\sigma_{22} = 146$  ppm and  $\sigma_{33} = 260$  ppm. Here, the line broadening was assumed to be 5 ppm in the simulation. The chemical shift tensor determined here will be used for the structural determination of the oriented components of PCL and PCL/ $\text{CaCO}_3$  compounds.

**Structural Analyses from <sup>13</sup>C NMR Carbonyl Peaks of the Oriented PCL/CaCO<sub>3</sub> Compounds with Draw Rate 100 mm/min**

Figure 5 shows the <sup>13</sup>C CP NMR spectra of carbonyl carbons of uniaxially drawn (100 mm/min at 50°C) sheets with different CaCO<sub>3</sub> content as a function of β<sub>L</sub>, the angle between the drawn direction and the magnetic field. The line shapes of the carbonyl carbon are slightly different between the PCL and PCL/CaCO<sub>3</sub> compounds. In particular, the carbonyl peaks of PCL/CaCO<sub>3</sub> compounds are slightly broader than those of PCL, especially, at both β<sub>L</sub> = 30° and β<sub>L</sub> = 60°. In addition, there were also little differences between the two kinds of PCL/CaCO<sub>3</sub> compounds (about 15 wt % and 35 wt %). The carbonyl peaks of the oriented component was slightly broadened with increasing CaCO<sub>3</sub> content. The simulated spectra (dot line) are also shown for the spectra of the carbonyl carbons with 35 wt % CaCO<sub>3</sub> (Fig. 6). The spectra with the powder pattern spectra subtracted from the observed spectra can be used for the simulation. The Euler angles α<sub>F</sub> and β<sub>F</sub> defined in our previous articles<sup>9,10</sup> were determined to be 10°

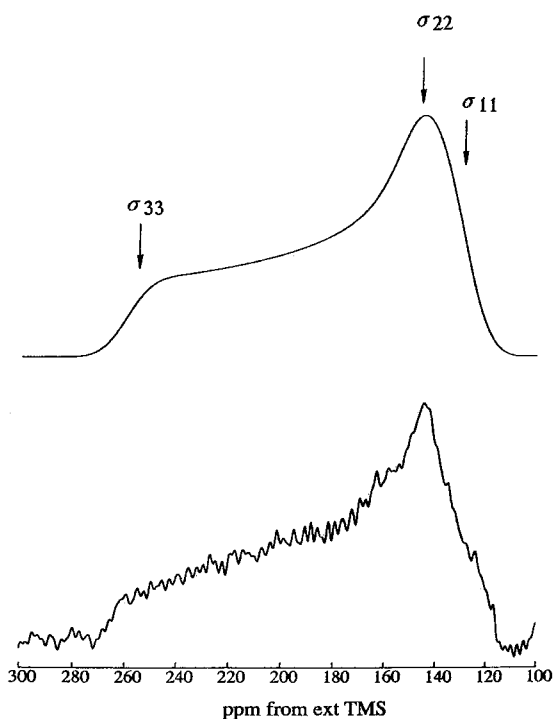


**Figure 4** The <sup>13</sup>C powder pattern spectra of carbonyl carbon of PCL powder (the observed spectrum (lower) and simulated one (higher)). The <sup>13</sup>C chemical shift tensors are determined as σ<sub>11</sub> = 128 ppm, σ<sub>22</sub> = 146 ppm and σ<sub>33</sub> = 260 ppm.

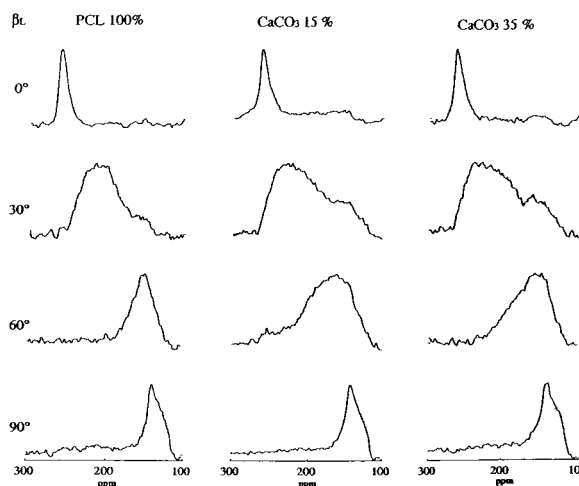


**Figure 5** The <sup>13</sup>C CP NMR spectra of carbonyl carbon uniaxially drawn (×4.5 at 50°C) PCL and PCL/CaCO<sub>3</sub> compounds (about 15 wt % and 35 wt %) as a function of β<sub>L</sub>, the angle between the draw direction and magnetic field.

and 5°, respectively, and the distribution parameter, *p*, determined by assuming Gaussian, was 13°. The structural parameters, α<sub>F</sub>, β<sub>F</sub>, and, *p*, for the oriented components obtained for uniaxially oriented PCL/CaCO<sub>3</sub> samples are summarized in Table I as well as the fraction of the oriented and unoriented components. Only the *p* value was changed and the α<sub>F</sub> and β<sub>F</sub> values remain constant. From the increasing *p* values as the CaCO<sub>3</sub> content increased, the oriented component of PCL/CaCO<sub>3</sub> compounds becomes more distributed than that of PCL. However, the average structure of the oriented components was kept constant.

**<sup>13</sup>C CP MAS NMR Spectra of Undrawn PCL/CaCO<sub>3</sub> Compounds**

Figure 7 shows the <sup>13</sup>C CP MAS NMR spectra of undrawn PCL and undrawn PCL/CaCO<sub>3</sub> samples (CaCO<sub>3</sub>; 15 wt % and 35 wt %, respectively). Any carbon peaks due to CaCO<sub>3</sub> could not be observed. The assignment of each peak has been reported.<sup>6</sup> The peaks of C<sub>1</sub>, C<sub>2</sub>, and C<sub>6</sub> carbons was split into two lines: the upfield line of C1 and C6 carbons and the downfield line of the C2 carbon have been assigned to the noncrystalline component, whereas the counterpart line of these carbons are ascribed to the crystalline component.

Figure 8 shows the expanded <sup>13</sup>C CP MAS NMR spectra of the carbonyl carbon of undrawn

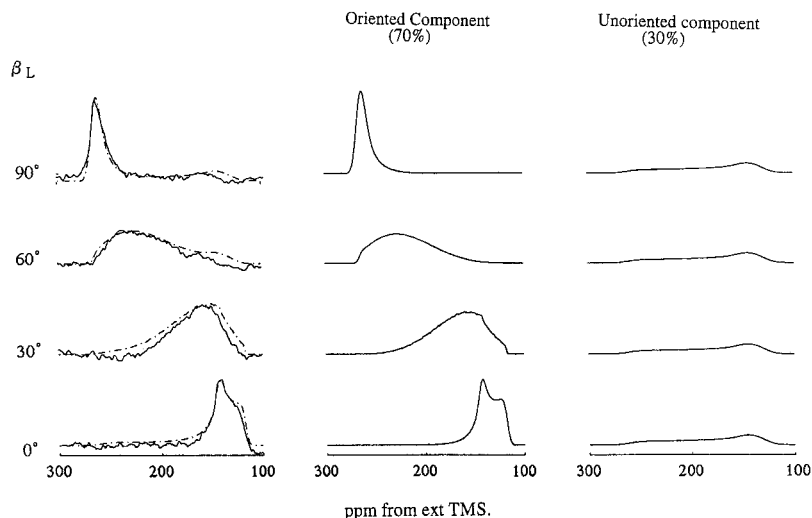


**Figure 6** The  $^{13}\text{C}$  CP NMR spectra of carbonyl carbon drawn ( $\times 4.5$  at  $50^\circ\text{C}$ ) PCL/ $\text{CaCO}_3$  sheet included 35 wt %  $\text{CaCO}_3$  as a function of  $\beta_L$ , the angle between the draw direction and magnetic field. Full and dotted curve shows observed and calculated spectra, respectively. The fraction of the two components, amorphous (30%) and oriented (70%) were determined by simulation. The spectral parameters were  $\alpha_F = 10^\circ$ ,  $\beta_F = 5^\circ$  and  $p = 13^\circ$ . When the chemical shift tensor are  $\sigma_{11} = 128$  ppm,  $\sigma_{22} = 146$  ppm and  $\sigma_{33} = 260$  ppm.

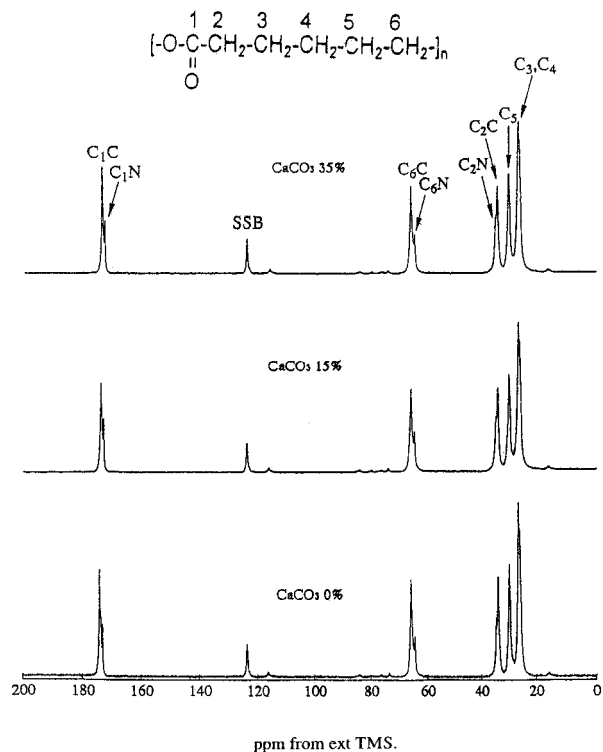
PCL and undrawn PCL/ $\text{CaCO}_3$  compounds (solid line) and the simulated spectra (dot line). By line shape analyses, the peaks were found to split into four peaks. Within the four peaks, the three peaks (I, II, III) at lower field were assigned to the crystalline components and the highest field peak IV to the noncrystalline component, respectively. The spectral patterns of the carbonyl carbon did not change with increasing  $\text{CaCO}_3$  for the undrawn samples. Therefore, it appears that the structural change of PCL did not occur even if  $\text{CaCO}_3$  was included.

Figure 9 shows the  $^{13}\text{C}$  CP NMR spectra of the carbonyl carbon (solid line) and the simulated spectra (dot line) of drawn PCL and PCL/ $\text{CaCO}_3$  samples ( $\text{CaCO}_3$ : 15 wt % and 35 wt %, respec-

**Table I** The Euler Angles,  $\alpha_F$ ,  $\beta_F$ , and Distribution of Fiber Axis,  $p$ , of Drawn PCL Specimens Including  $\text{CaCO}_3$  Particles

$\text{CaCO}_3$	0	15	35
$p$ ( $^\circ$ )	8	13	13
$\alpha_F$ ( $^\circ$ )	10	10	10
$\beta_F$ ( $^\circ$ )	5	5	5
Oriented component (%)	90	80	70

The fraction of oriented component is also listed.



**Figure 7**  $^{13}\text{C}$  CP MAS NMR spectra of undrawn PCL and undrawn PCL/ $\text{CaCO}_3$  compounds (about 15 wt % and 35 wt %).

tively) with draw rate of 100 mm/min. The spectra of drawn PCL and PCL/CaCO<sub>3</sub> samples changed dramatically with increasing CaCO<sub>3</sub> content. In the line-shape analyses, the four peaks observed for undrawn samples were also observed in these cases. In these drawn sheets, peak I disappeared when CaCO<sub>3</sub> was blended with PCL. And peak II also decreased with increasing the CaCO<sub>3</sub> content from 41% to 9–11%. In contrast, the intensities of peaks III and IV increased with increasing the CaCO<sub>3</sub> content from 21 to 34% and from 18 to 33–36%, respectively. The width of peak IV became broader with increasing CaCO<sub>3</sub> content. Peak IV corresponds to the amount of the powder component used in the <sup>13</sup>C CP NMR analysis (Table I). Peak IV is the amorphous phase, and increased in the drawn PCL/CaCO<sub>3</sub> samples. In addition, a new peak, labeled V, was observed in the drawn PCL/CaCO<sub>3</sub> samples. At present, structural discrimination of these peaks (I, II, III, and V), which were assigned to crystalline structure could not be performed exactly, but it appears that when the PCL that had been blended with CaCO<sub>3</sub> particles was exposed under shear stress, some structural change occurred. The com-

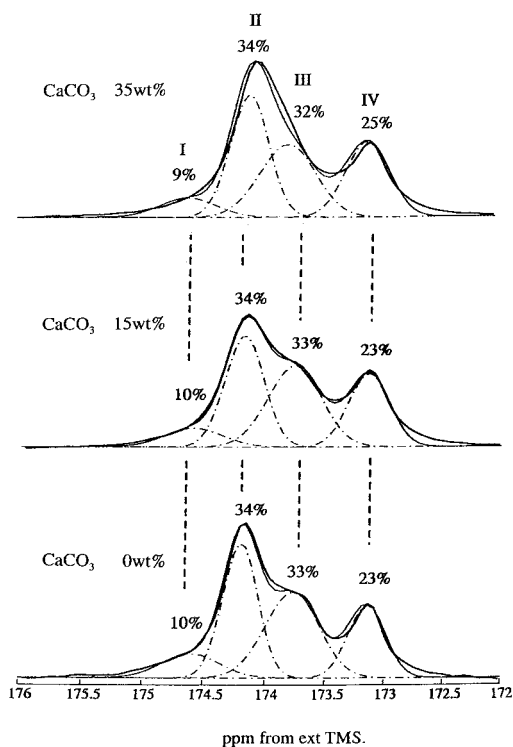


**Figure 8** <sup>13</sup>C CP MAS NMR spectra of carbonyl carbon of undrawn PCL and undrawn PCL/CaCO<sub>3</sub> compounds and their deconvolution spectra into four fraction (I, II, III, IV, and V).

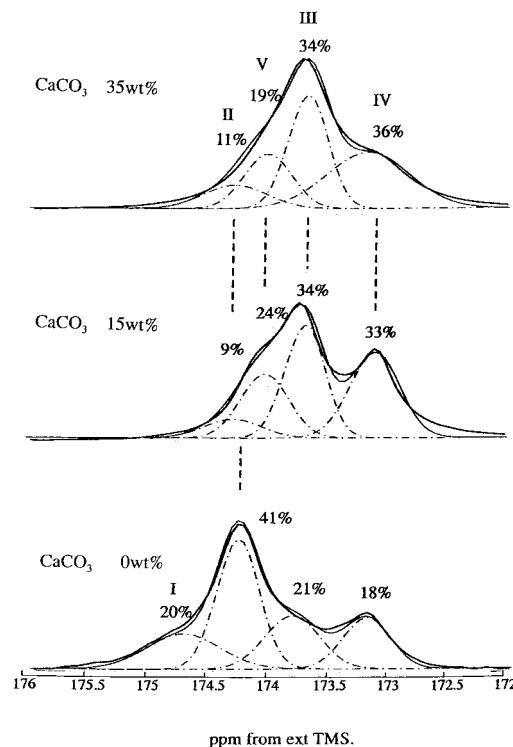


**Figure 9** <sup>13</sup>C CP MAS NMR spectra of carbonyl carbon of drawn PCL and drawn PCL/CaCO<sub>3</sub> compounds and their deconvolution spectra into five fraction (I, II, III, IV, and V).

position ratio of each fractions are also described in Figure 9.

**CONCLUSION**

The loss elasticity, *E''* (Fig. 2) shows almost the same curve for both of the undrawn sheets [Fig. 2(a)] and the drawn sheets [Fig. 2(b)] as a function of CaCO<sub>3</sub> content. In contrast, the storage modulus, *E'*, of drawn PCL/CaCO<sub>3</sub> samples increased nonlinearly with increasing CaCO<sub>3</sub> and this curve showed lower *E'* values than those of undrawn samples. Therefore, some physical changes occurred under shear stress as a result of the process for PCL/CaCO<sub>3</sub> compounds.

By the simulation of <sup>13</sup>C CP NMR spectra, one oriented component and one unoriented component was obtained in both undrawn samples and drawn samples. In this case, it is difficult to separate more two components; thus, the oriented component was treated as the mean structure of several oriented components. Also, the distribution parameter, *p*, of the oriented component of

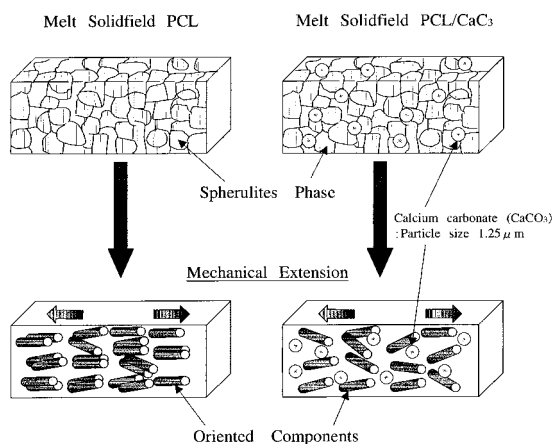


**Figure 10** Diagrammatic arrangement of oriented component and amorphous region in uniaxially oriented PCL and uniaxially oriented PCL/CaCO<sub>3</sub> compound.

drawn PCL/CaCO<sub>3</sub> compounds was 13°, which is larger than those (8°) of drawn PCL sample. Therefore, it is clear that adding CaCO<sub>3</sub> particles to PCL and drawing uniaxially, the arrangement of the oriented component was distributed.

From the line shape analyses of <sup>13</sup>C CP MAS NMR spectra, four peaks were obtained in not only undrawn samples but also the drawn samples of PCL and PCL/CaCO<sub>3</sub> compounds. However, the line-shape patterns are different between undrawn samples and drawn samples. Although, for the undrawn samples, structural change did not occur within the four peaks with respect to the CaCO<sub>3</sub> content, dramatic structural changes occurred in the drawn samples. In the case of drawn samples, peaks I and II disappeared and/or decreased with CaCO<sub>3</sub> content and drawing; at the same time, peak III increased and a new peak, V, appeared in drawn PCL/CaCO<sub>3</sub> samples. In addition, peak IV, which was assigned to the amorphous component, increased,

and peak shape become broader with increasing CaCO<sub>3</sub> content.

From these result, the phenomena that was observed in the storage elastic modulus, *E'* [Fig. 1(b)] may be explained. In the CaCO<sub>3</sub> compounds, the arrangement of the oriented component was disturbed and the structure of the oriented component changed under the shear stress of the drawing process (Fig. 10). Therefore, in this PCL/CaCO<sub>3</sub> system, the physical properties are strongly dependent on the oriented structures, which was formed under shear stress of the drawing process.

T.A. acknowledges support from Bio-oriented Technology Research Advancement Institution.

## REFERENCES

1. Scott, G.; Gilead, D., Eds. *Biodegradable Polymer. Principal and Application*; Chapman & Hall: London, 1995.
2. Hollinger, J. O., Eds. *Studies in Polymers Science 12, Biomedical Application of Synthetic Biodegradable Polymer*, CRC Press: Boca Raton, FL, 1995.
3. Bittiger, H.; Marchessault, R. H. *Acta Crystallogr* 1970, B26, 1923.
4. Chatani, Y.; Okita, Y.; Tadokoro, H.; Yamashita, Y. *Polym J* 1970, 1, 555.
5. Hu, H.; Dorset, D. L. *Macromolecules* 1990, 23, 4604.
6. Kaji, H.; Horii, F. *Macromolecules* 1997, 30, 571.
7. Guillermo, J.; Nobuo, O.; Hidekazu, K.; Takashi, O. *J Appl Polym Sci* 1997, 64, 2211.
8. Renstad, R.; Karlsson, S.; Sandgren, A.; Albertsson, A. C. *J Environ Polym Degrad* 1998, 6, 209.
9. Asakura, T.; Konakazawa, T.; Demura, M.; Ito, T.; Maruhashi, Y. *Polymer* 1996, 37, 1965.
10. Ito, T.; Maruhashi, Y.; Demura, M.; Asakura, T. *Polymer* 2000, 41, 859.
11. Nicholson, L. K.; Asakura, T.; Demura, M.; Cross, T. A. *Biopolymers* 1993, 33, 847.